CONF-890703--18

"The submitted manuscript has been authored by a contractor of the U.S. Government under contract No. DE-AC05-84OR21400. Accordingly, the U.S. Government retains a nonexclusive, royalty-free license to publish or reproduce the published form of this contribution, or allow others to do so, for U.S. Government purposes."

Extraction induced emittance growth for negative ion sources*

J. H. Whealton, P. S. Meszaros, R. J. Raridon, K. E. Rothe,
Oak Ridge National Laboratory, Oak Ridge, Tennessee 37831

CONF-890703--18

DE89 017586

Abstract

Nonlinear emittance growth produced by ion extraction is considered by a 3-D analysis in a Vlasov-Poisson-Boltzmann formulation. Phenomena considered include: (1) presheath effects, including electron depletion, (2) electron sheath accumulation (for large transverse magnetic fields), (3) nonlinear sheath fields (obtained by a self-consistent solution with an assumed quasi-equilibrium positive ion distribution and at least one Vlasov distribution), (4) nonlinear fringe fields produced by the accelerator-extractor itself (obtained self-consistently with item 3 above, (5) nonlinear space charge of the beam itself, and (6) beam in conjunction with extracted electrons. For specific volume negative ion source configurations, an investigation of the contribution of aberrations caused by an electron trap and electron accumulation in the extraction sheath are studied. Either of these effects can contribute significantly to the beam emittance, possibly dominating the contribution of the negative ion temperature in the source.

DISCLAIMER

This report was prepared as an account of work sponsored by an agency of the United States Government. Neither the United States Government nor any agency thereof, nor any of their employees, makes any warranty, express or implied, or assumes any legal liability or responsibility for the accuracy, completeness, or usefulness of any information, apparatus, product, or process disclosed, or represents that its use would not infringe privately owned rights. Reference herein to any specific commercial product, process, or service by trade name, trademark, manufacturer, or otherwise does not necessarily constitute or imply its endorsement, recommendation, or favoring by the United States Government or any agency thereof. The views and opinions of authors expressed herein do not necessarily state or reflect those of the United States Government or any agency thereof.

*Research sponsored by the Exploratory Studies Program of the Oak Ridge National Laboratory, operated for the U.S. Department of Energy by Martin Marietta Energy Systems, Inc., under contract DE-AC05-84OR21400.

MASTER

DISTRIBUTION OF THIS DOCUMENT IS UNLIMITED

Negative ion sources are the basic ingredient of neutral beam injectors of energy greater than 200 kV. There are many applications of this technology: e.g., (1) injection of neutral beams into high density plasma confinement devices to provide auxiliary heating and, in the case of tokamaks, current drive, and (2) injection of energy from a distance into targets in a vacuum. Previously, the state-of-the-art tools for negative ion accelerator design are like those for positive ion sources 20 years ago. As with positive ion sources, improvement is possible if a validated tool can be developed to actually design extractors and preaccelerators.

We have proposed a phenomenological description of space-charge imbalance in a negative ion source presheath. This is identified as a principal source of difference between the apparent inscrutability of negative ion source extraction optics compared to positive ions. For positive ion extraction sheaths, particularly at low magnetic fields, the plasma electrons are available to instantly and completely (on the order of kT/e) cancel any excesses of positive ion space charge that might occur just before extraction. The properties of this nonlinear sheath in many cases are well known. However, for negative ion sources the situation is different. Electrons are extracted or hit a wall before being affected by space-charge fluctuations. Only the positive ions are present to cancel the space-charge imbalance.

This description is coupled with a full multidimensional, nonlinear Vlasov-Poisson analysis which includes nonlinear field effects, space-charge effects, and image charges. With this approach, we believe that many of the heretofore unexplained differences between negative and positive extraction optics will be brought to light. We have effectively modeled intense volume negative ion sources with respect to transverse space charge limits and RMS emittance production. We compare the theoretical treatment and the experimental data taken at the Los Alamos National Laboratory[1] (LANL). We also make some theoretical observations on an injector proposed by Lawrence Berkeley Laboratory (LBL).[2]

We consider in detail the geometric configuration of a negative ion source at LBL.[2] If we compute the total output current as a function of plasma density, then we arrive at Fig. 1. We see that for low values of the current density, j (cases A and B), there is a linear increase in output current. For extremely low values of the current (case A), we see a slight rise above this linear value. The prototypical case for low values of current density is illustrated in Fig. 2 (b), where only the ions inside the geometrical shadow of the extraction electrode are extracted and pass through the

accelerator. For the case of extremely low densities, we have the situation as typified in Fig. 2 (a). In this situation, some of the ions outside of the shadow of the extraction plasma electrode enter the extraction region due to the presheath fields, which occur as fringe fields of the applied potentials.

For sufficiently high current density, as shown in case (c) of Fig. 2, we have a transverse space-charge limitation, where the ions are impinging upon the extraction electrode. This is denoted as the first transverse space-charge limit. For yet higher values of the current density, shown by Fig. 2 (d), the onset of the second space-charge limit is reached. Here the ions now intercept the electron filter electrode. For an increase in plasma density, the net current decreases. This is what is meant by a transverse space-charge limit. In this case, the transverse space charge is determined principally by the small bore of the extraction electrode. The space-charge limit of this accelerator is approximately 130 mA (H^-). This value might exceed the current density capability of the ion source, which would indicate the space-charge limit is not a practical inhibition upon the performance of the accelerator. However, the aberrations present below the space-charge limit may be. For positive ion extraction, the space-charge limit appears at approximately 270 mA, as shown in Fig. 1.

The RMS transverse emittance of the beam is examined and the results shown in Fig. 3. Here we see a wild behavior: we begin with a rather high emittance value at very low densities, then we go to a very low value at slightly higher plasma densities, and then steadily increasing to a much higher value and finally sharply decreasing again, but not to as low a value as before. This erratic behavior is fully explained and can be understood by reference to Figs. 2 (a)-(d). Very low densities, indicated by point (a) in Fig. 3, are shown in Fig. 2 (a). Here the ions have a very nonlinear force applied to them which produces significant beam halo or aberrations. These ions were tricked out of hitting the plasma electrode by the presheath fringe fields, due to the applied electrostatic accelerator potentials. As shown in the figure, the outside trajectories are crossing over neighboring interior trajectories. This produces a relatively high transverse RMS emittance, such as indicated in Fig. 3. However, for case (b) in Fig. 3, where the emittance is minimum, the sheath for negative ion extraction produces relatively small aberrations of the beam, as seen in Fig. 2 (b). For yet higher densities near the first space-charge limit, the emittance rises, and the outside trajectories, due to the fringe fields at the electron trap, cross over significantly the penultimate trajectories, producing a highly aberrated beam. The design of the electron trap has not been made with

respect to minimizing the beam transverse emittance at maximum achievable current, but only with respect to trapping electrons. Also, the electron trap was designed assuming that the sheath was at the same plane as the exit aperture. There is no evidence to support this conjecture. If we increase the density still further, then we see a decrease in the emittance, as in case 3 (d). Even though we are beyond the first and second space-charge limits, the electron trap is vignetting the worst trajectories on the outside, thereby eliminating them from the emittance measurement.

Next, we analyzed the experimental data of Ralph Stevens and colleagues of LANL using an LBL-type negative ion source. This two-dimensional analysis for the nonlinear negative ion extraction sheath shows promising results, at least in the zero temperature limit. Examples of the agreement between the subject analysis and the experiments are indicated in Fig. 4. Here, we show negative ion current as a function of inverse perveance for a space-charge dominated case. The analysis is indicated by the solid line and the experimental-based determinations by the symbols. Using this analysis, ion trajectories and equipotential contours are shown by solid and dashed curves respectively in Figs. 5-7; the four cases shown correspond to the cases A-D indicated in Fig. 4. In Fig. 5 are shown four different perveance beams in the Stevens negative ion source (labeled a-d). The desirable operating regime is most closely represented by the one labeled (b). This perveance is near, but slightly less than, the transverse space-charge limit of this accelerator. Notice that even near the space-charge limit, there is still significant field penetration in the plasma at the sheath for ion extraction. For lower perveance, as shown in the top part, Fig. 5 (a) the beam crosses over and intercepts the extraction electrode. The field penetration is very significant, and the beam is extremely aberrated. This is not a useful mode of operation. Figure 5 (c) shows a perveance which is significantly higher than the transverse space-charge limit. Here the ions are shown to be intercepting the extraction electrode. If one were to increase the plasma density in the source, the number of ions that would hit the electrodes would increase faster than those that would actually exit the ion source. Thus the higher the source plasma density, the lower the extracted current which gets accelerated. This is illustrated in Fig. 5 (d). In Figs. 6-7, a blowup of the sheath region is featured. Here, we see a significant amount of field penetration [Fig. 7 (a)] as well as space-charge limited perveance [Fig. 7 (d)]. So, we have for the same geometric configuration both field penetration and space-charge limit.

A preliminary three-dimensional analysis of this same source follows. We studied the RMS transverse emittance for extraction from the negative ion source at LBL. In Fig. 8, we show the negative ion source extraction sheath featured in Fig. 5, but in full three-dimensions. A calculation of the entire geometry is shown in Fig. 9, where the region of Fig. 8 (a) is indicated. In Fig. 8 (a), the extraction sheath is symmetric; however, in Fig. 8 (b), we have included the effect of the electron space charge of those electrons which are in an $E \times B$ guiding-center drift across the sheath, on their way out of the ion source. Here we see the sheath as asymmetric with potential contours as shown. This oblique sheath and the nonlinear aberrations associated with it give rise to an additional RMS emittance of the beam. The oblique electron contribution is shown in Fig. 10 showing this cause of emittance growth to be possibly significant.

References

1. R. Stevens, private communication 1987.

2. K. Leung, private communication 1988.

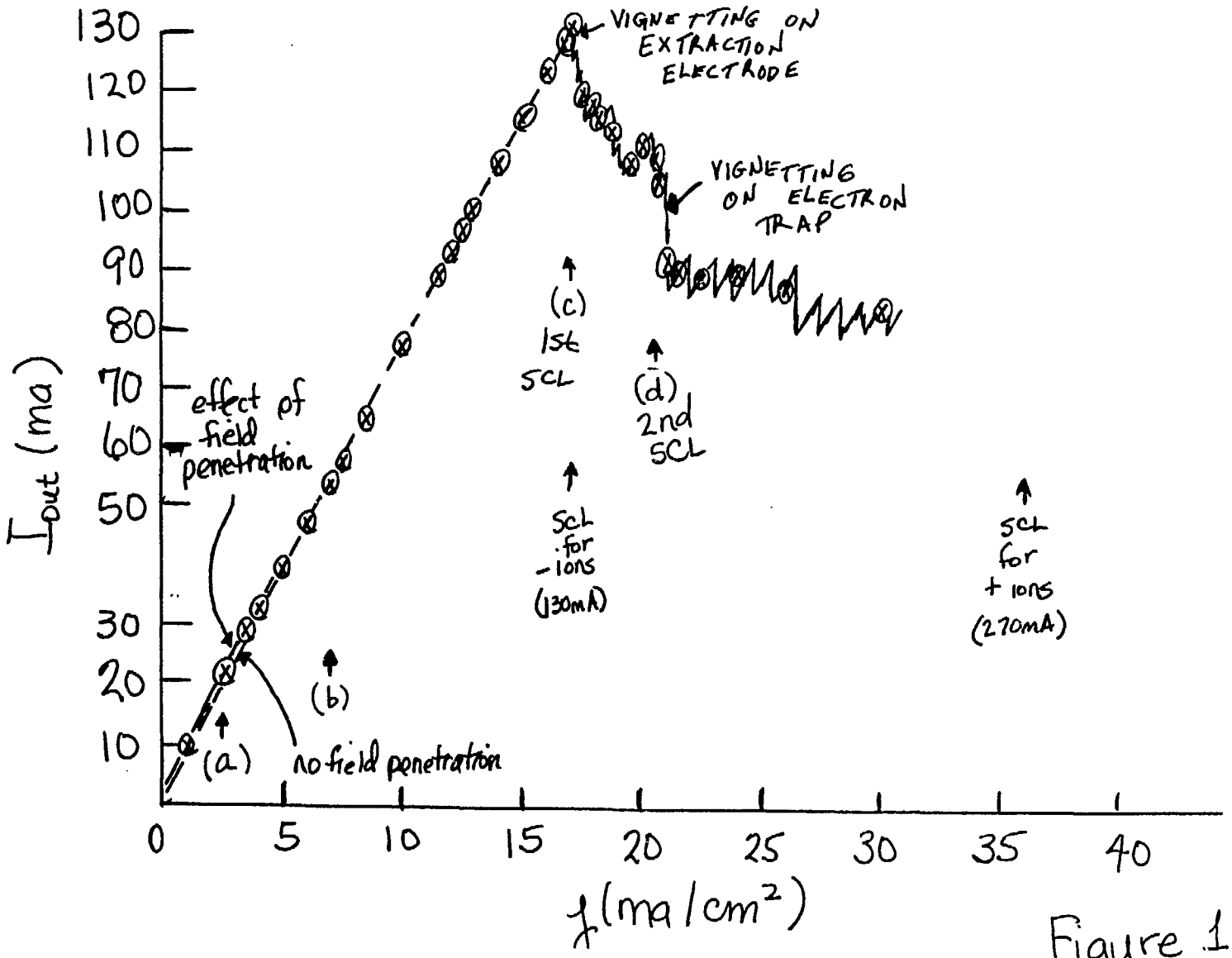

Figure 1

Output current vs. Plasma Density

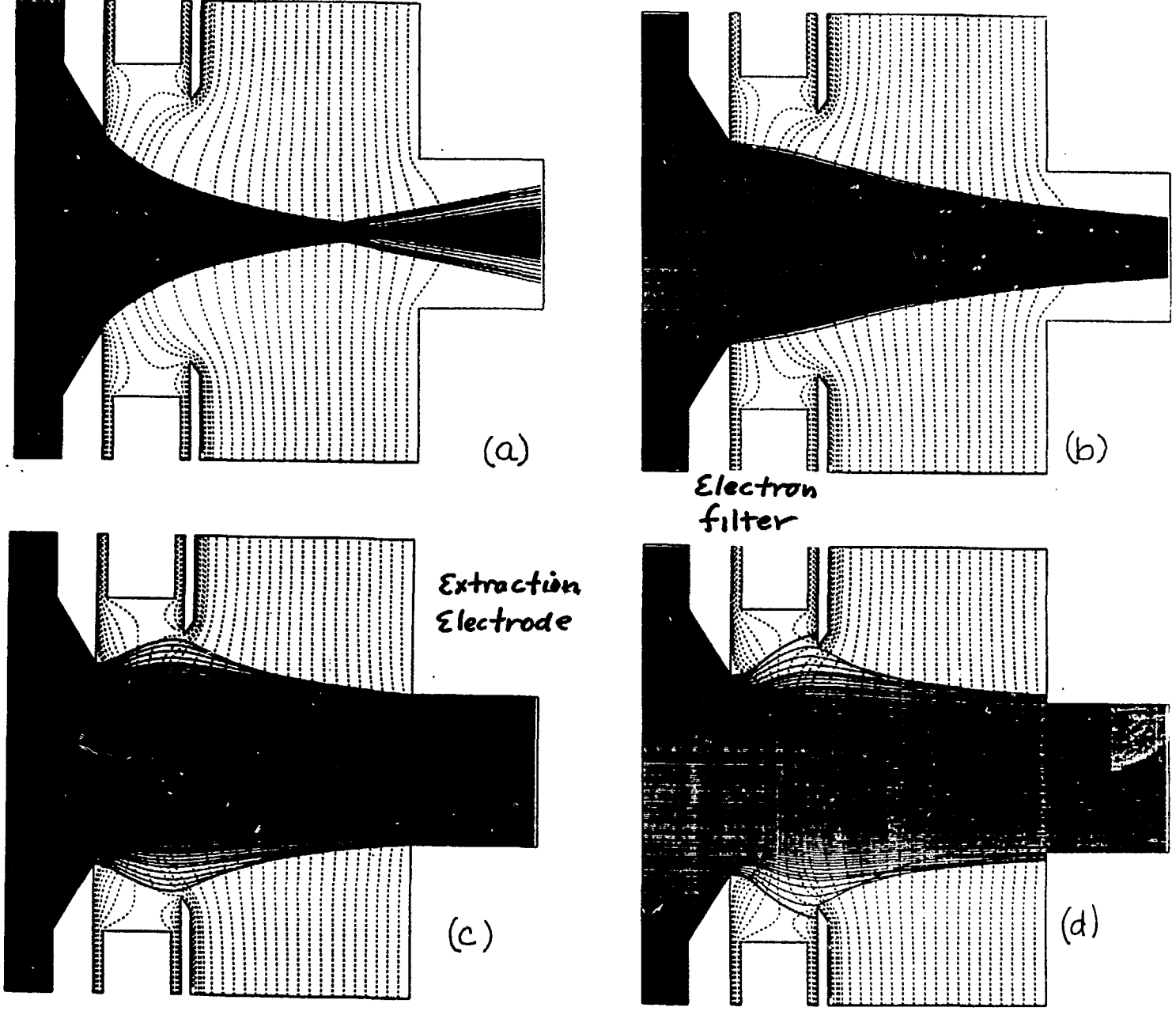

ION EXTRACTION

FIGURE 2

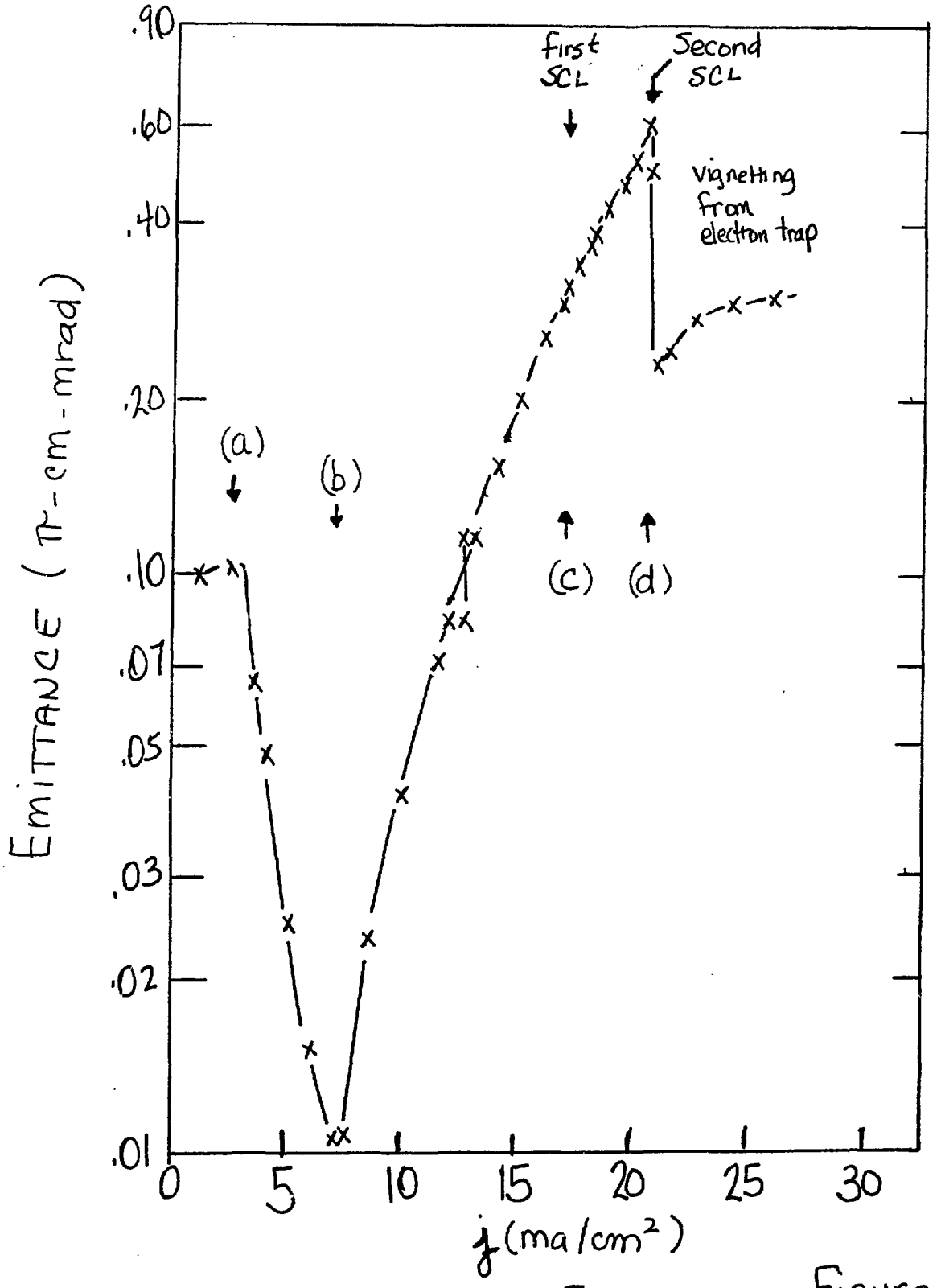

RMS Transverse Emittance

Figure 3

ORNL-DWG 88-3194 FED

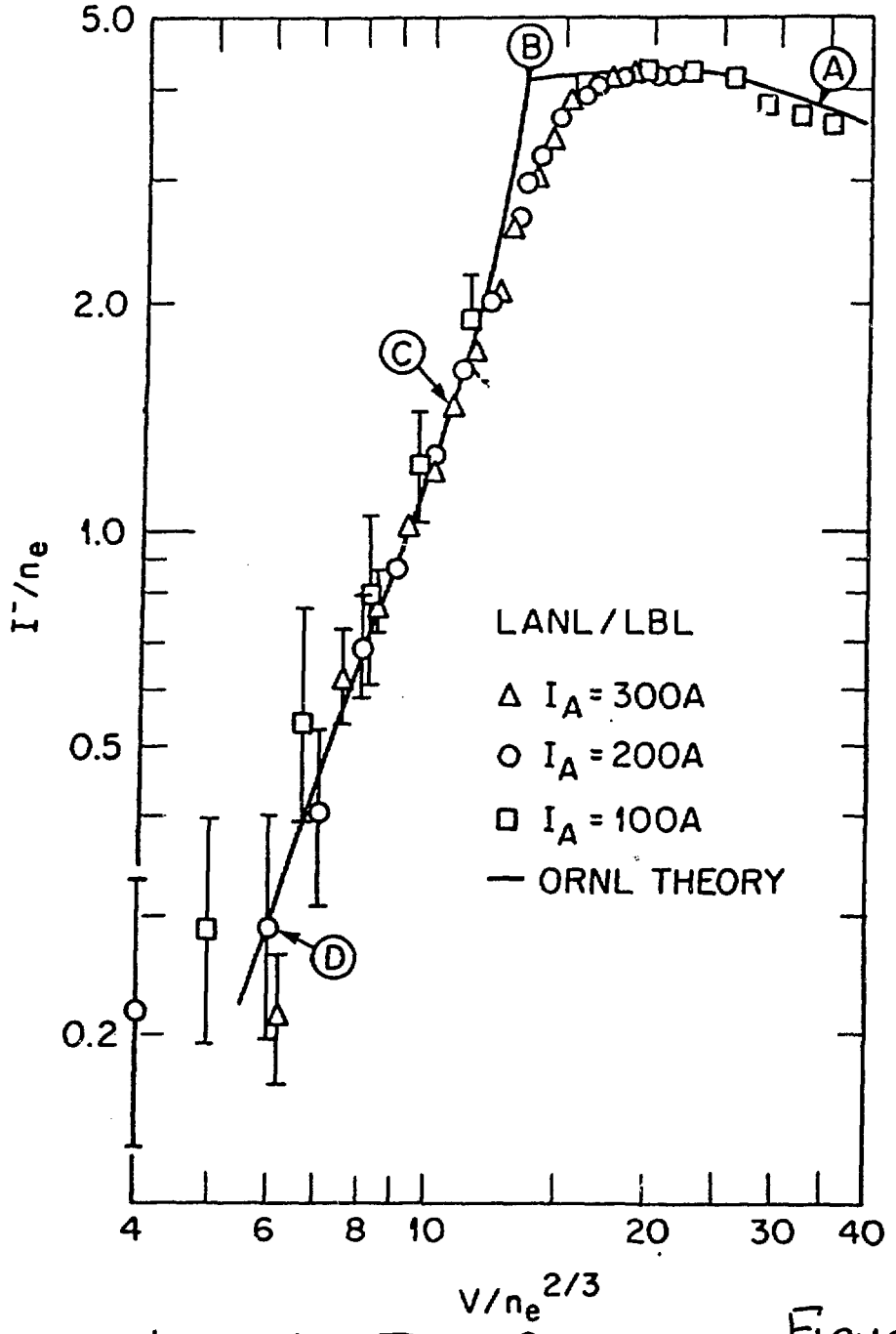

Negative Ion Current vs. Inverse Perveance

Figure 4

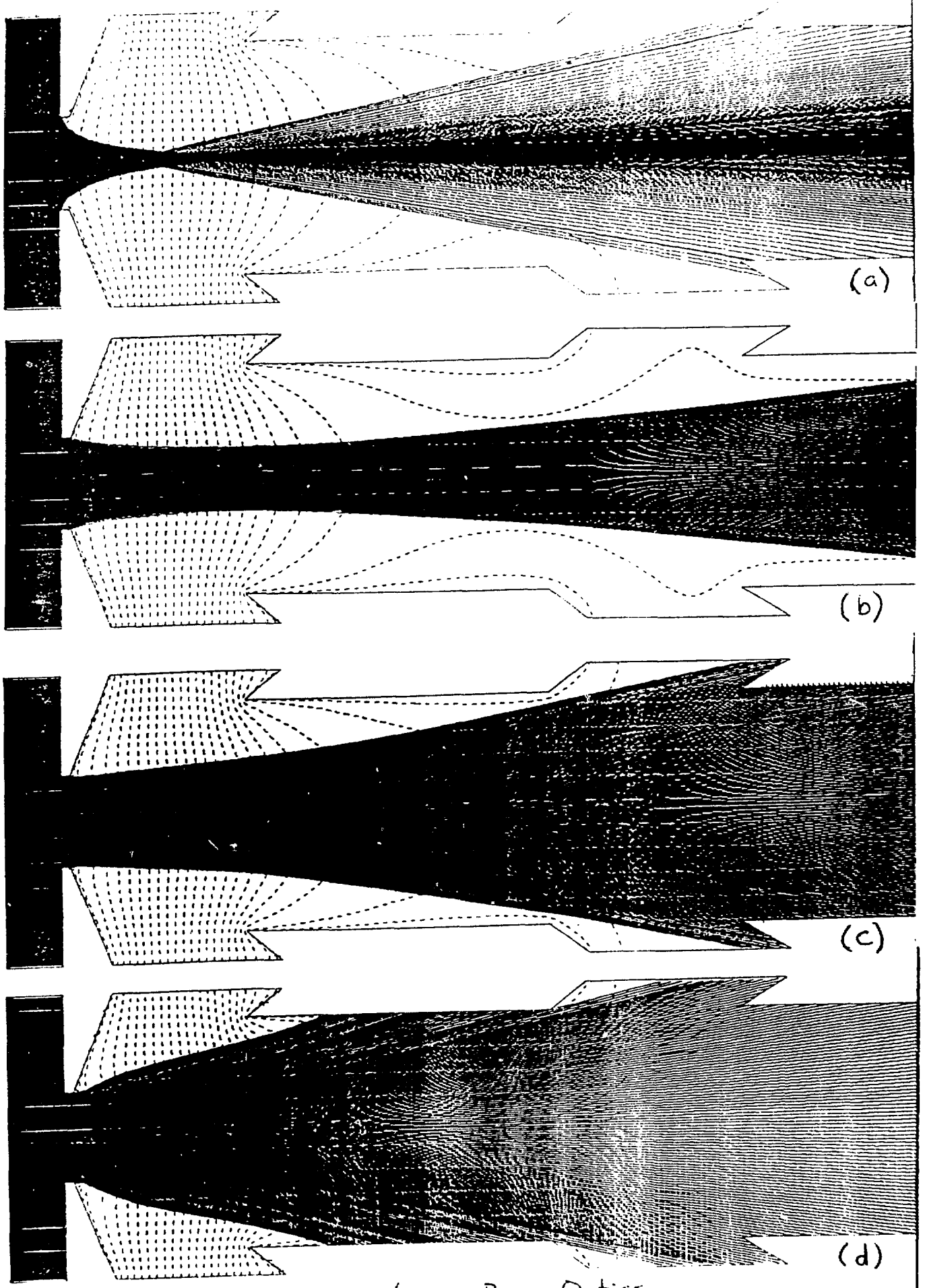
(a)
(b)
(c)
(d)

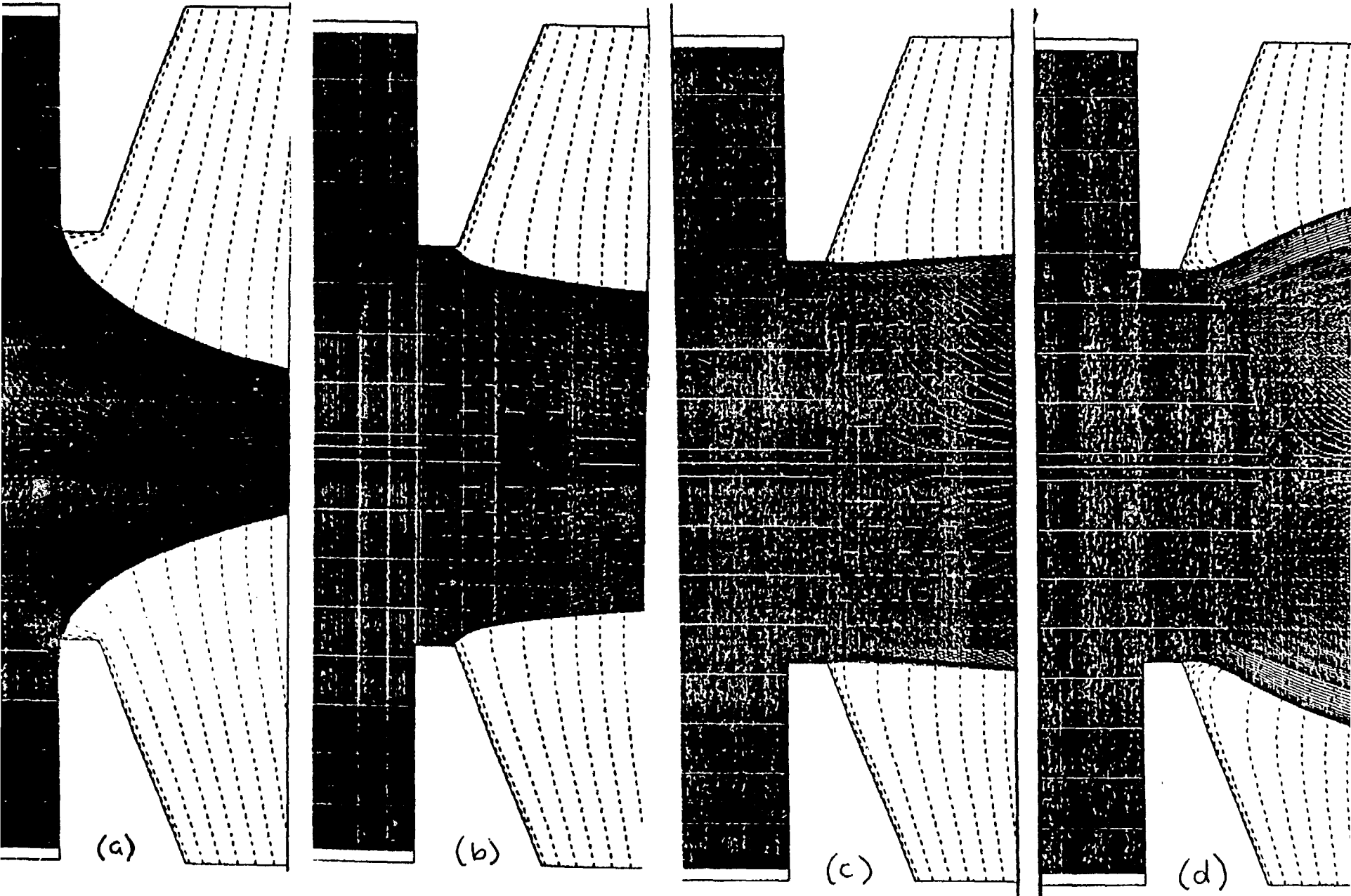

Figure 6 Blowup of LANL/LBL beam optics

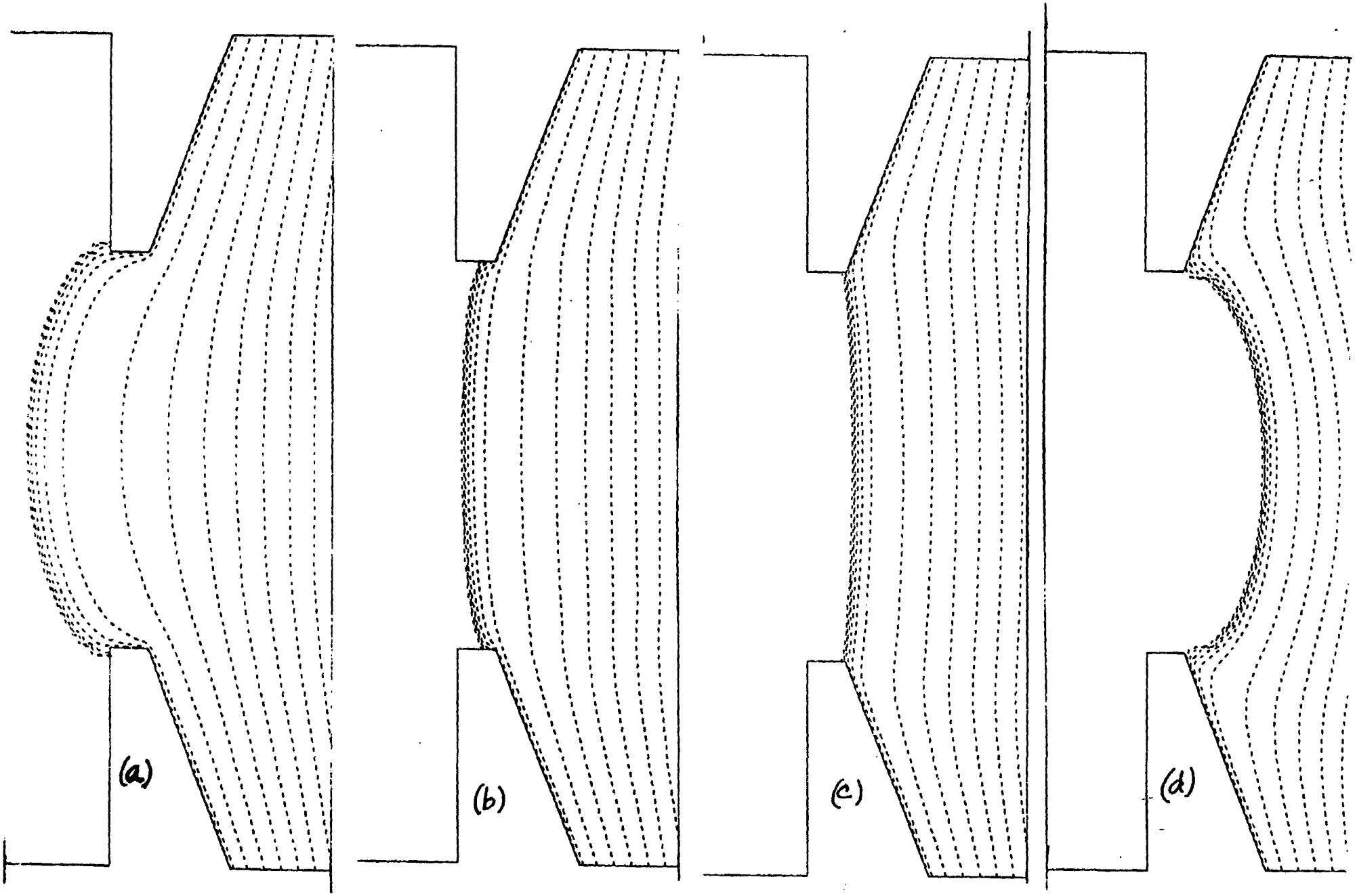
(a)
(b)
(c)
(d)

SIDE VIEW

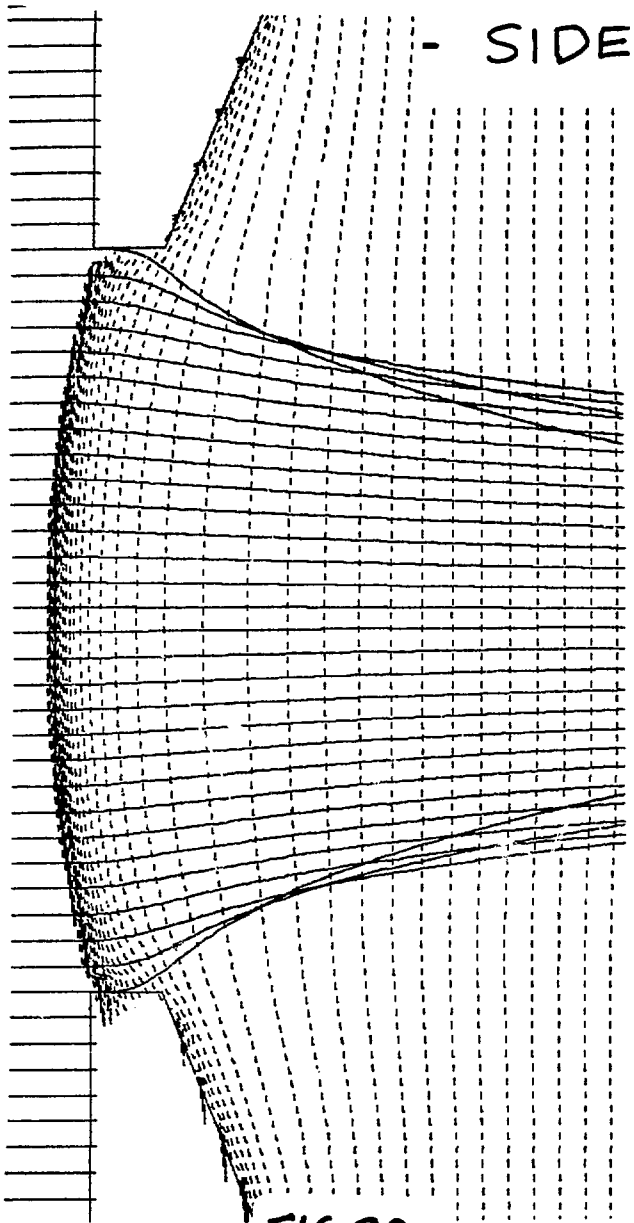

FIG 8A

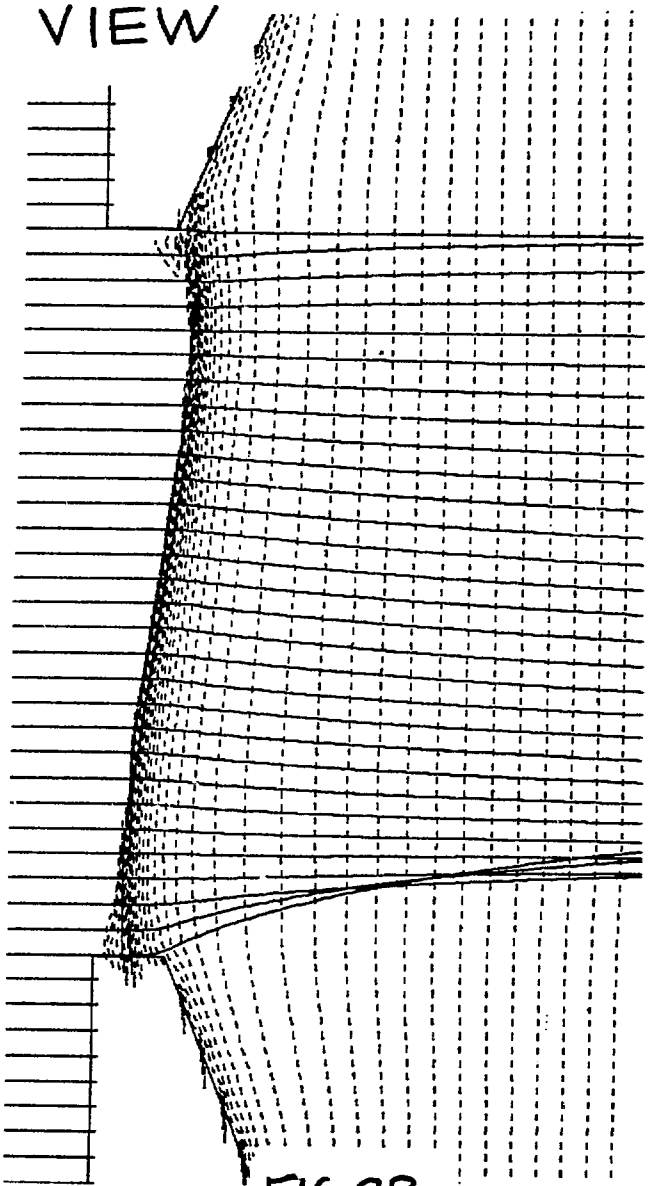

FIG 8B

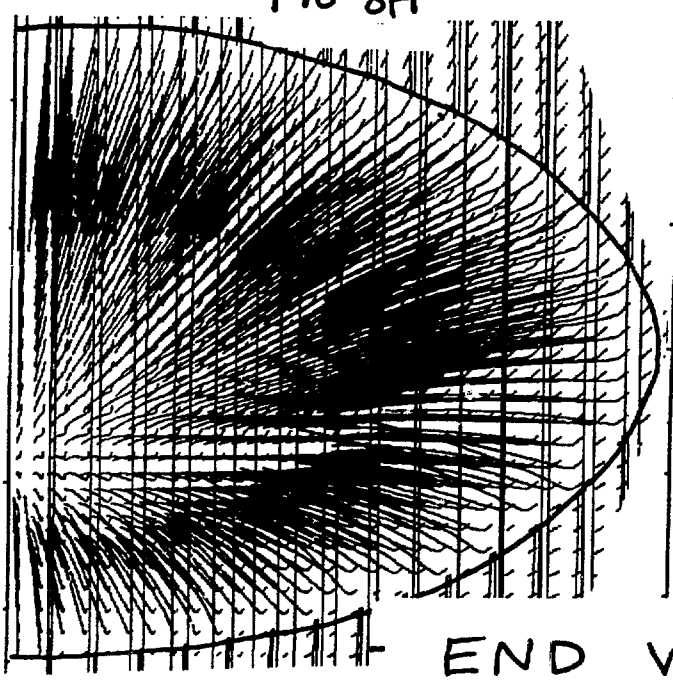

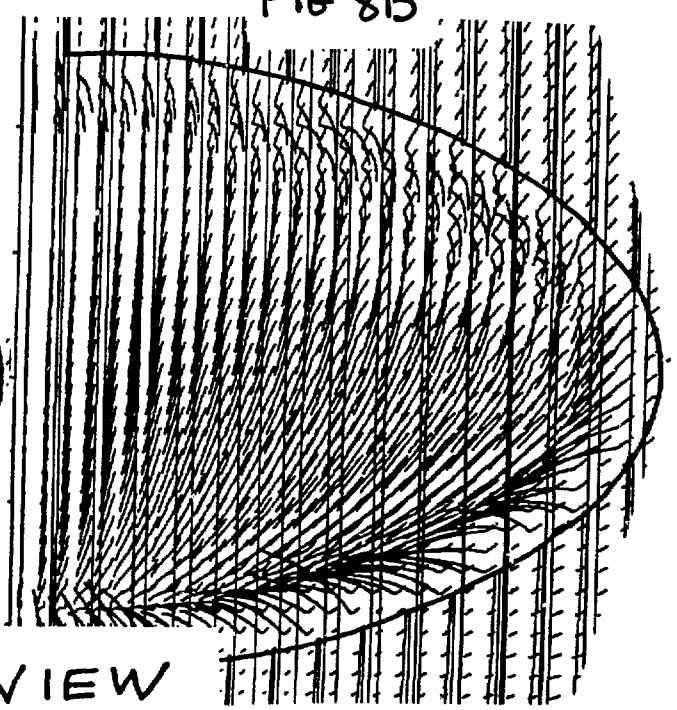

END VIEW

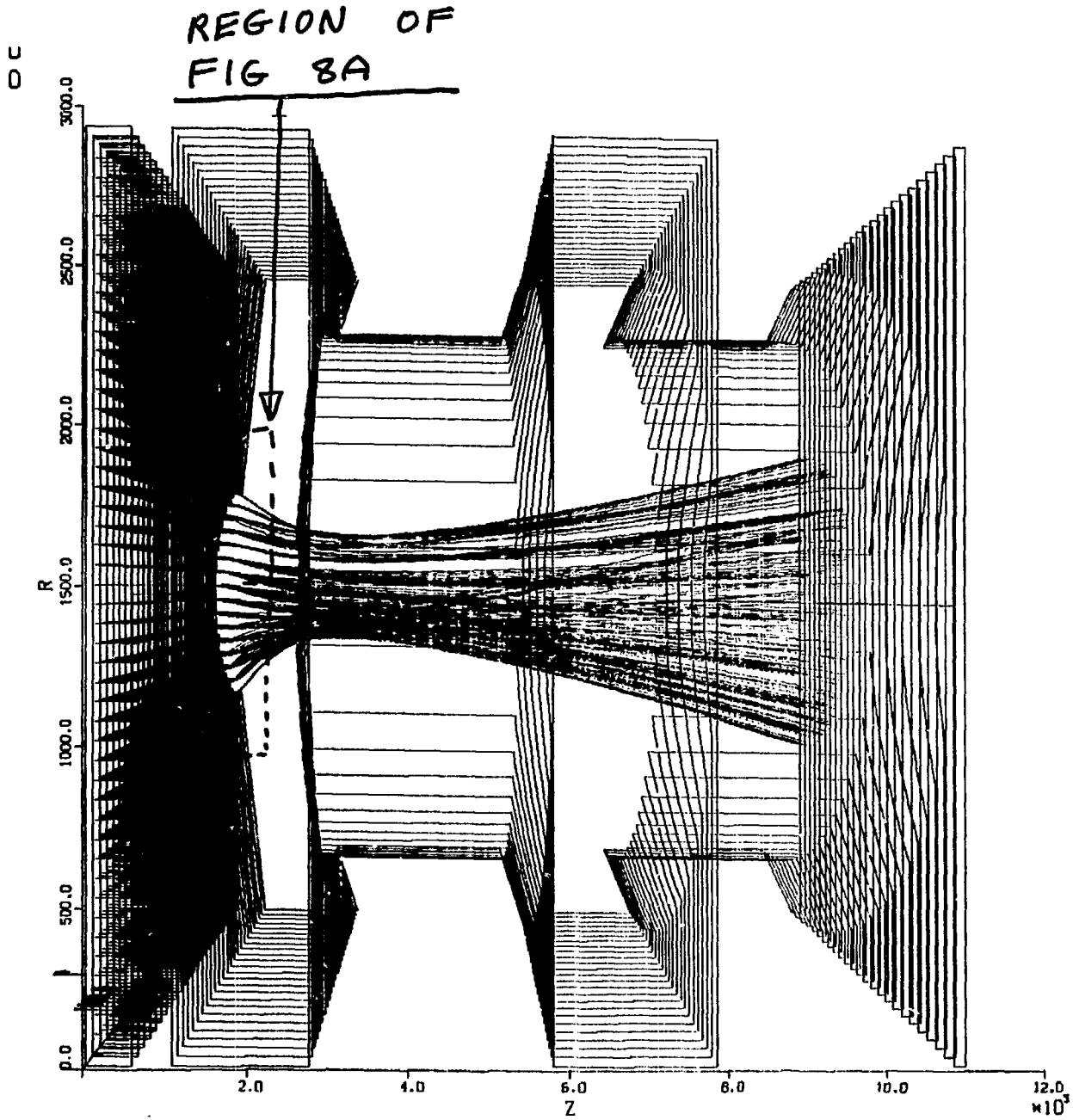

3-D Calculation of LBL Source

Figure 9

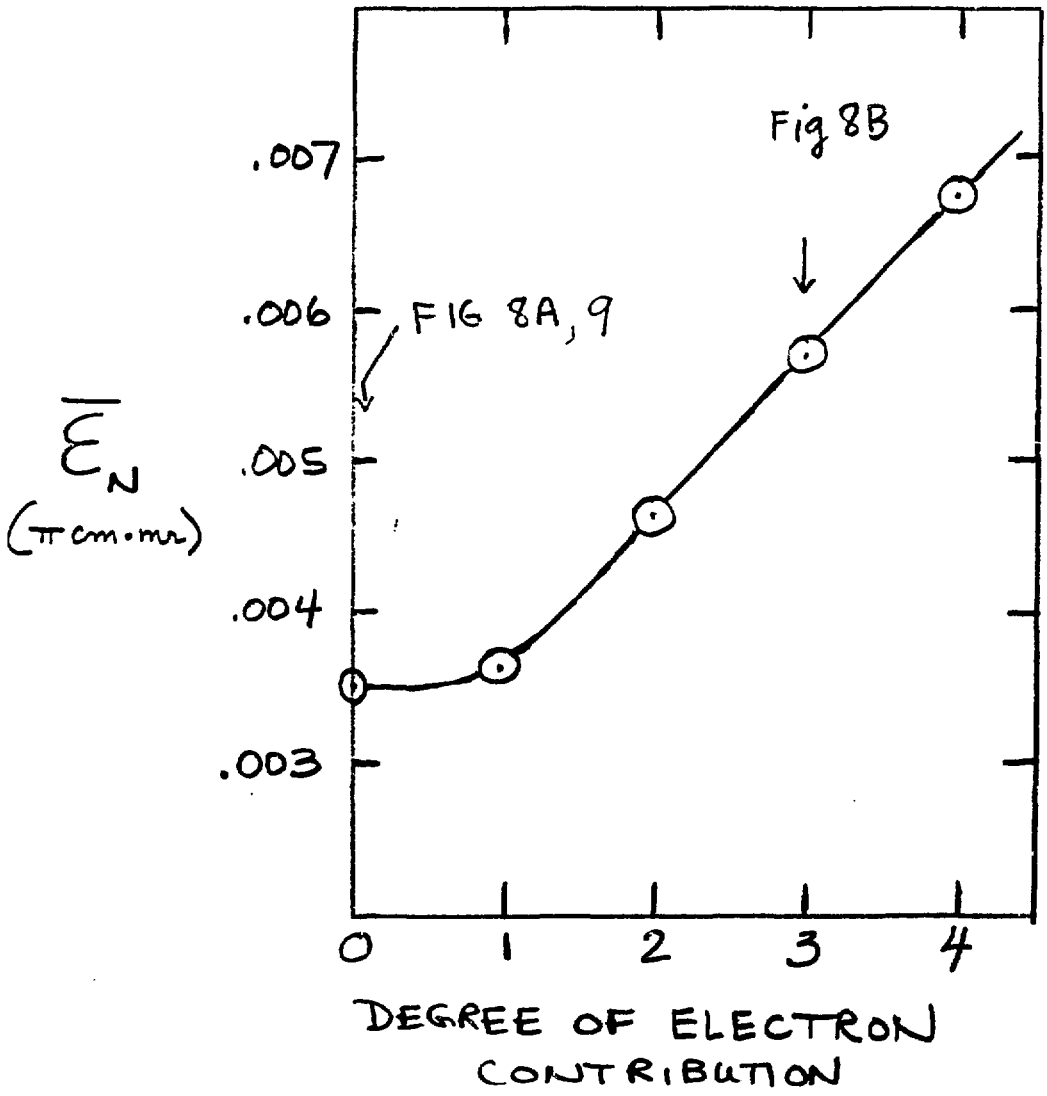
Fig 8B
FIG 8A, 9
.007
.006
.005
.004
.003
$\overline{\varepsilon}_N$
(π cm·mr)
0
1
2
3
4
DEGREE OF ELECTRON
CONTRIBUTION

FIG 10.